SCIENCE CHINA
Information Sciences

Supplementary File

Frequency Scaling and Elastic Transition in HF-VHF WS2 NEMS Resonators

Jiankai Zhu[1,2,#], Chenfei Lv[1,#], Ziluo Su[1,#], Bo Xu[1], Fei Xiao[3,*] Hao Jia[2,*] & Zenghui Wang[1,*]

[1]*Institute of Fundamental and Frontier Sciences, University of Electronic Science and Technology of China, Chengdu 610054, China*

[2]*State Key Laboratory of Transducer Technology, Shanghai Institute of Microsystem and Information Technology, Chinese Academy of Sciences, Shanghai 200240, China*

[3]*Hangzhou Institute of Technology, Xidian University, Hangzhou 311200, China*

#These authors contributed equally
*Corresponding author (email: xiaofei@xidian.edu.cn, hao.jia@mail.sim.ac.cn, zenghui.wang@uestc.edu.cn)

For a circular drumhead resonator with both non-zero tension and bending rigidity, the fundamental mode resonance frequency f_0 can be expressed as [Ref. 5 in the Main Text]:

$$f_0=\left(\frac{(kr)}{2\pi}\right)\sqrt{\frac{D}{\sigma r^4}\left[(kr)^2+\frac{\gamma r^2}{D}\right]}. \tag{S1}$$

Here, $\sigma=\rho t$ is the drumhead's areal mass density (ρ: volumetric mass density), γ (in N/m) is the 2D tension in the drumhead (force per unit length). $D=E_Y t^3/[12(1-v^2)]$ is the flexural rigidity, with E_Y, t, and v being the Young's modulus, thickness, and Poisson's ratio, respectively. (kr) is a mode-dependent parameter determined numerically.

In the limit of $\gamma r^2/D\rightarrow 0$, the second term in Eq. 1 becomes negligible, leaving the resonance frequency governed solely by the first term — that is, the resonator operates in the mechanical "plate limit." In this case, Eq. S1 becomes

$$f_0=\frac{(k_2 r)^2}{2\pi r^2}\sqrt{\frac{D}{\sigma}}, \tag{S2}$$

which corresponds to the ideal circular plate, where the resonance frequency is determined by the bending rigidity D and is independent of the tension γ. Moreover, in the limit of $\gamma r^2/D\rightarrow 0$, the value of ($kr$) can be approximated as 10.215 [Ref. 5 in the Main Text]. Therefore, Eq. S2 can be further approximated as:

$$f_0\approx\frac{10.215}{2\pi}\sqrt{\frac{E_Y}{12\rho\left(1-v^2\right)}}\frac{t}{r^2}. \tag{S3}$$

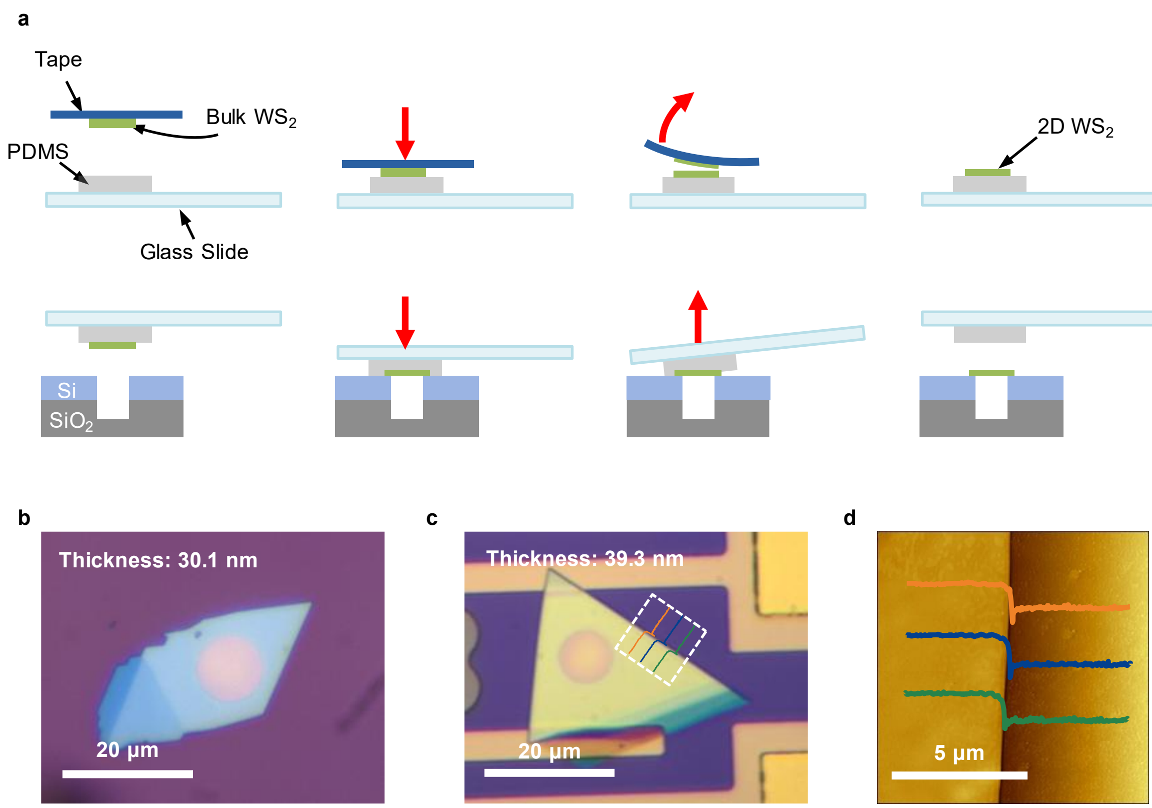

Figure S1. Device transfer, device-structure images, and AFM measurements. (a) Schematic of the exfoliation and dry transfer process. (b) Optical image of the device without electrode structures. The 2D material is directly transferred onto a SiO_2 substrate, forming a single contact interface (SiO_2/WS_2) that improves the transfer yield and efficiency. (c) Optical image of the device with electrode structures. The 2D material is transferred onto a substrate with pre-patterned electrodes, enabling the electrical excitation configuration shown in Fig. S2. (d) AFM measurement of a representative device. The measurement area is indicated by a white dashed box in the (c). Notably, the actual device images (Figs. S4-S6) show pre-patterned electrodes with different geometries, yet all are wired following the same configuration as in Fig. S2. These devices can also be optically excited, and when the laser power is carefully controlled to avoid significant photothermal effects, their resonant responses are nearly identical to those under electrical excitation (Fig. S7). In addition, optical images of the devices (Figs. 2, S4–S6) reveal that some thinner devices exhibit wrinkles, leading to nonuniform tension distribution—regions with pronounced wrinkles generally experience higher tension, while other areas may have lower tension. The pretension extracted using Eq. 1 represents an equivalent value obtained under the assumption of a uniform in-plane stress distribution. Even for devices exhibiting wrinkles, this value can be reliably used to predict the resonant frequency ranges of devices with different sizes and to analyze their electro-tuning potential.

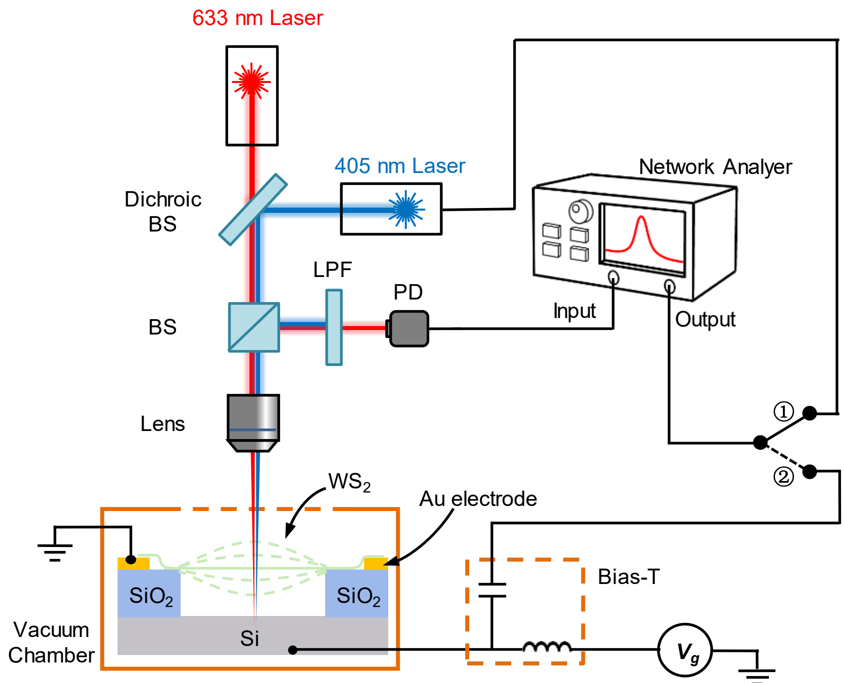

Figure S2. Schematic of our custom-built resonance measurement setup. Different measurement configurations can be realized for detecting resonances with optothermal excitation (Switch ① closed) and electrical excitation (Switch ② closed). PD: Photodetector; BS: Beam Splitter; LPF: Long-Pass Filter. When Switch ① is closed, the 405 nm laser intensity is periodically modulated by the AC signal from the Network Analyzer, producing a periodic optothermal effect on the 2D drumhead and driving its vibration. When Switch ② is closed, the 405 nm laser is turned off, and the AC signal together with a DC bias is applied to the gate via a bias-T. Since the drumhead is grounded through the metal electrode, the back gate (heavily doped Si substrate) induces a periodic capacitive electrostatic force on the drumhead. All devices are operated under vacuum (~1×10^{-4} Torr) at room temperature. Notably, under optothermal excitation, we carefully control the laser power to avoid heating effects, and the measured resonance responses are nearly identical to those under electrostatic actuation (Fig. S7).

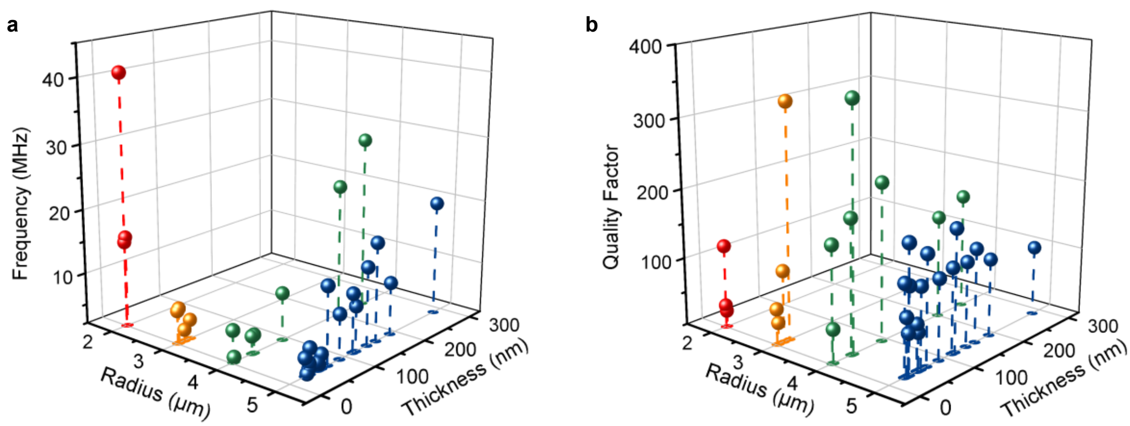

Figure S3 Performance of all the WS_2 nanomechanical resonators. (a) Measured fundamental mode resonance frequency f_0 and (b) quality factor (Q) as functions of device radius and thickness (number of layers). Device radiuses are color coded: red (2 μm), orange (3 μm), green (4 μm), and blue (5 μm).

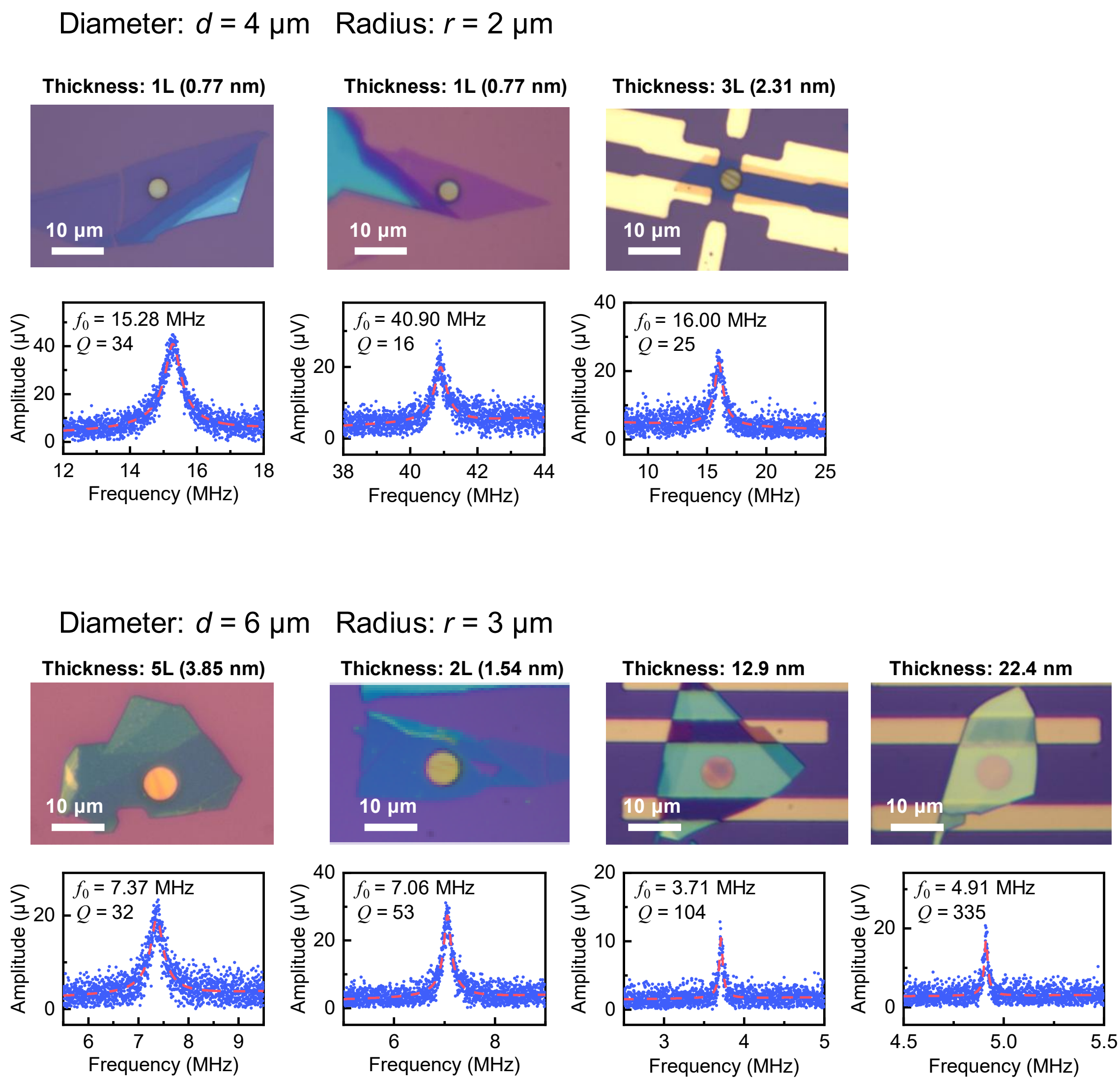

Figure S4 Optical microscopy images and optothermally excited resonance responses of WS_2 resonators with a radiuses of 2, 3 μm. Blue points represent the measured data and red dashed lines show the corresponding fits to the simple harmonic oscillator (SHO) model. Extracted resonance frequencies f_0 and quality factors Q are labeled in the panels.

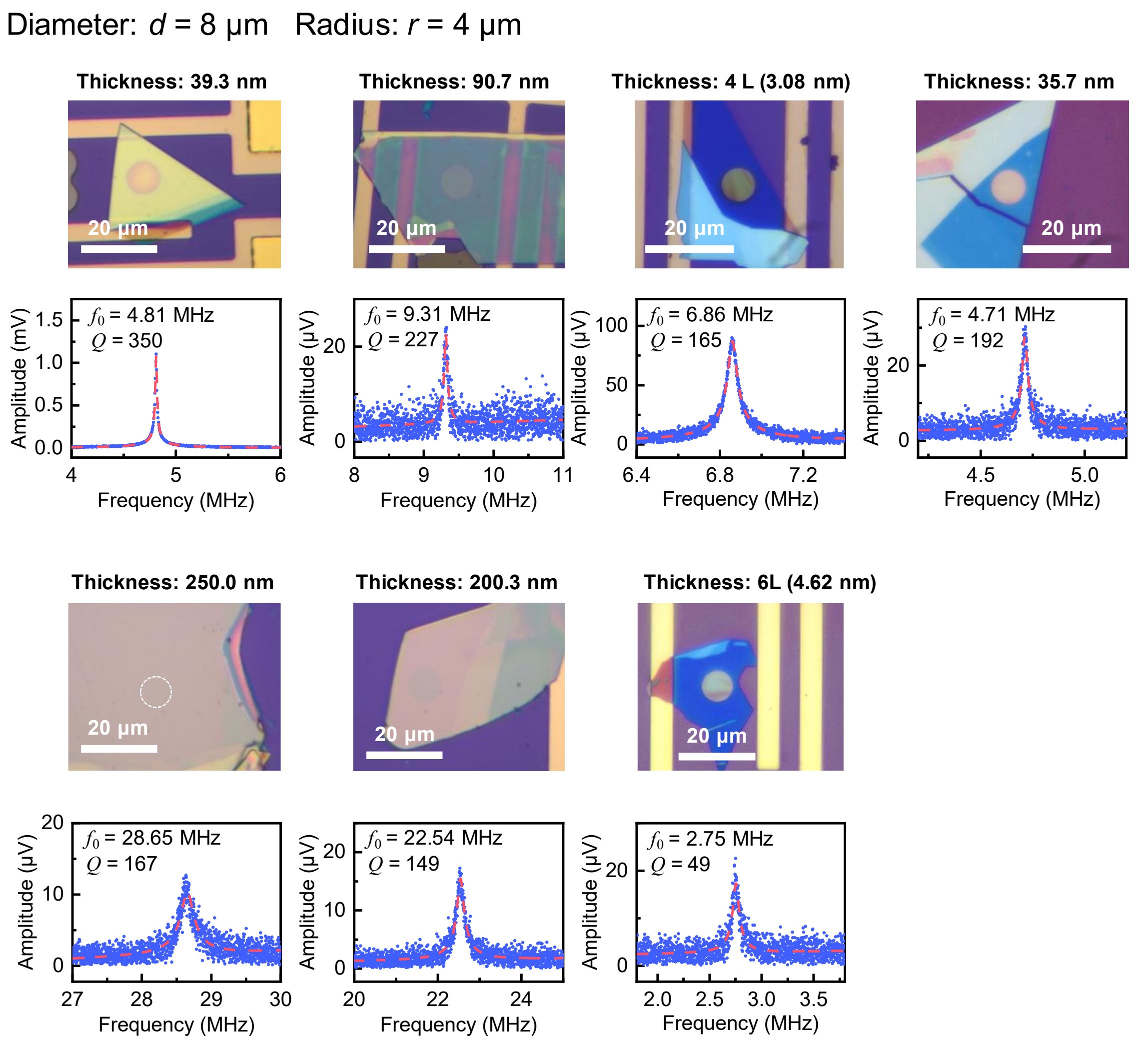

Figure S5 Optical microscopy images and optothermally excited resonance responses of WS_2 resonators with a radius of 4 μm. Blue points represent the measured data and red dashed lines show the corresponding fits to the simple harmonic oscillator (SHO) model. Extracted resonance frequencies f_0 and quality factors Q are labeled in the panels.

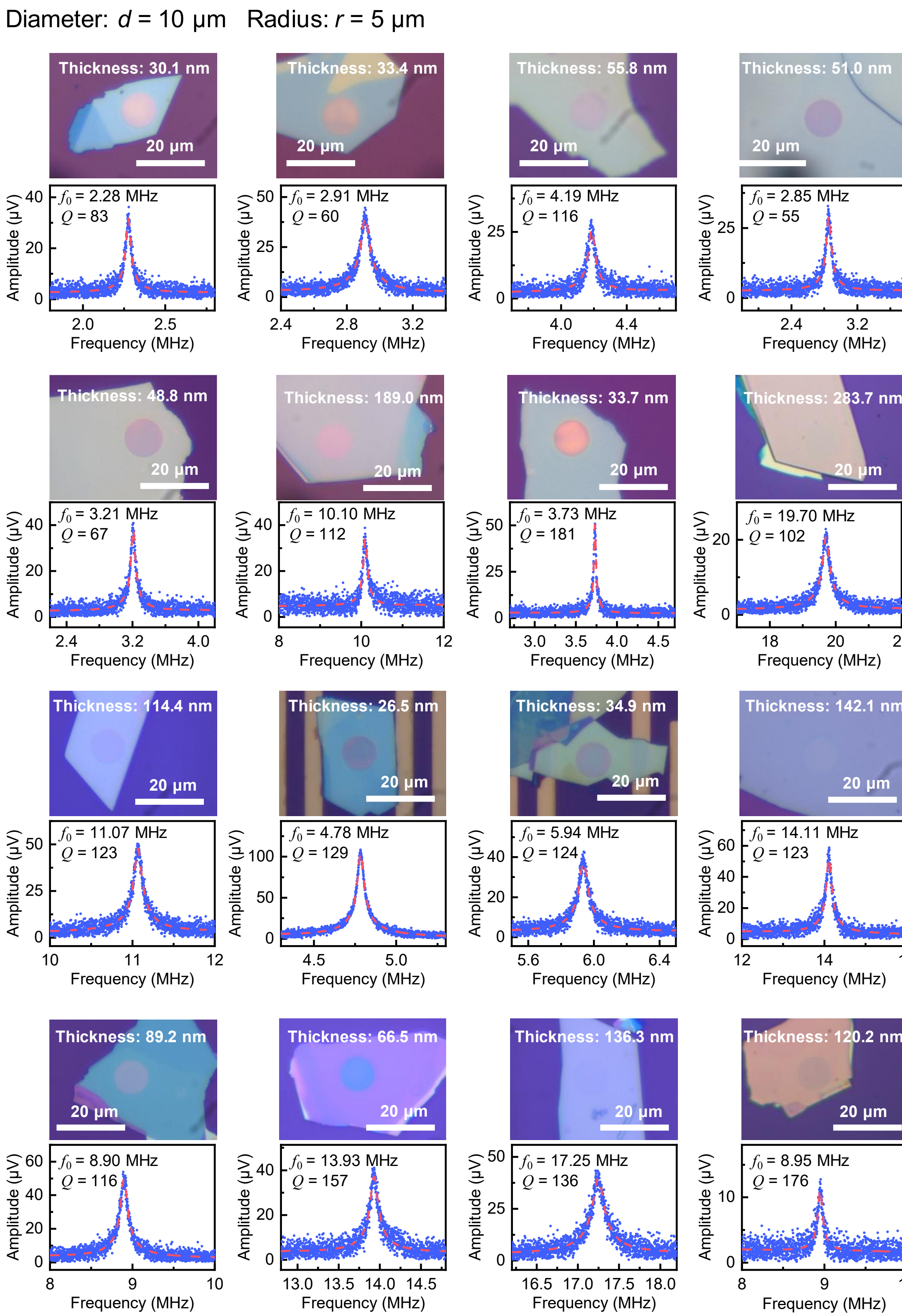

Figure S6 Optical microscopy images and optothermally excited resonance responses of WS_2 resonators with a radius of 5 μm. Blue points represent the measured data and red dashed lines show the corresponding fits to the simple harmonic oscillator (SHO) model. Extracted resonance frequencies f_0 and quality factors Q are labeled in the panels.

Device #	Device radius (µm)	Resonance Frequency f_0 (MHz)	Quality Factor Q	Number of Layers	Thickness (nm)	Thickness/Radius² (m^{-1})
1	4	4.81	350	52	39.3	2456
2*	4	9.31	227	118	90.7	5671
3	5	2.28	83	39	30.1	1203
4	5	2.91	60	43	33.4	1336
5	5	4.19	116	72	55.8	2232
6	5	2.85	55	66	51.0	2041
7	5	3.21	67	63	48.8	1952
8*	5	10.10	112	245	189.0	7560
9	5	3.73	181	44	33.7	1347
10*	5	11.07	123	149	114.4	4575
11	5	4.78	129	34	26.5	1062
12	5	5.94	124	45	34.9	1396
13*	5	14.11	123	185	142.1	5685
14*	5	8.90	116	116	89.2	3568
15	5	13.93	157	86	66.5	2659
16*	5	17.25	136	208	160.0	6401
17*	5	8.95	176	156	120.2	4809
18*	5	19.70	102	368	283.7	11348
19	4	6.86	165	4	3.08 (Raman)	193
20	4	4.71	192	46	35.7	2232
21	4	2.75	49	6	4.62 (Raman)	289
22*	4	28.65	167	325	250.0	15625
23*	4	22.54	149	260	200.3	12521
24	3	7.37	32	5	3.85 (Raman)	428
25	3	7.06	53	2	1.54 (Raman)	171
26	3	3.71	104	17	12.9	1436
27	3	4.91	335	29	22.4	2491
28	2	15.28	34	1	0.77 (Raman)	193
29	2	40.90	121	1	0.77 (Raman)	193
30	2	16.00	25	3	2.31 (Raman)	578

Table S1. List of all measured WS_2 resonators with device parameters. Thickness determination: For few-layer samples (≤10 layers), the layer number is determined via low-frequency Raman spectroscopy. For thicker samples, atomic force microscopy (AFM) provides more reliable estimates. Notably, for thicker samples, the layer number can only be estimated within an approximate range and should not be considered exact.

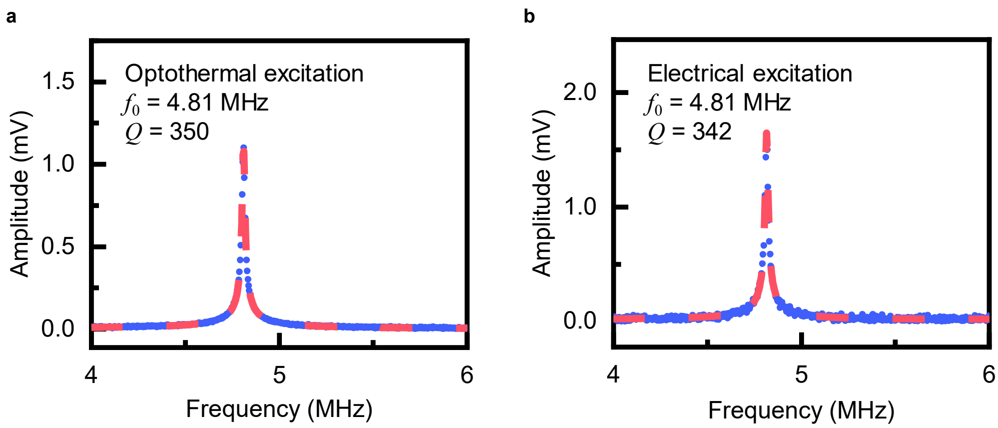

Figure S7 The amplitude-frequency response curves obtained through (a) optothermal excitation or (b) electrical excitation, along with their fitting results. Blue points represent the measured data, and red dashed lines show the corresponding fits to the simple harmonic oscillator (SHO) model. Extracted resonance frequencies f_0 and quality factors Q are labeled in the panels.